



# SUSTAINABLE COOK STOVE - MODELING AND DESIGN

Sibley School of Mechanical and Aerospace Engineering, Cornell University

Junxing Lu, Haolun Fan

5/12/2014

## Table of Contents

1 Introduction.....	2
2 Development of Model .....	4
2.1 Simplification to 2-D Axisymmetric Geometry.....	4
2.2 Geometry .....	6
2.3 Mesh .....	8
2.3.1 Uniform Mesh.....	8
2.3.2 Refined Mesh.....	8
2.4 Material Properties and Boundary Conditions .....	9
2.5 Heat Source (Chemical Reaction).....	11
2.5.1 Uniform Heat Source .....	11
2.5.2 Time Dependent Heat Source .....	12
2.5.3 Local Temperature Dependent Heat Source .....	14
2.5.4 Local Temperature and Mass Fraction Dependent Heat Source (Char Formation) .....	15
2.5.5 Future Coding Direction .....	18
3 Simulation Results and verification .....	19
3.1 Mesh sensitivity check.....	19
3.2 Parameter specification.....	20
3.3 Simulation results .....	22
3.4 Heat Source verification .....	23
4 Optimization .....	26
4.1 Objectives .....	26
4.2 Approaches .....	27
4.2.1 Filling.....	27
4.2.2 Insulating & adding fins.....	28
4.2.3 Adding heating effect & contact resistance.....	30
4.2.4 Adding convection on the top wall .....	31
4.2.5 Ceramic insulation .....	32
4.3 Design Recommendation .....	34
4.4 Future Improvement of the Model .....	34
References .....	35
Division of works .....	36

## 1 Introduction

All around the world, in spite of the difference of technology and wealth, people use different type of stoves to prepare their food. Accordingly, fuel sources vary from stove to stove. However, most cases involve one of these energy sources: gas, electricity and biomaterial.

What about a stove uses more than one source? Would it be more fuel efficient? At Cornell, students designed and manufactured a Cook-Stove that uses heat from ordinary combustion to cook as well as to facilitate pyrolysis reaction, which, in turn, generates gas that becomes part of the fuel. To achieve this function, our Cook-Stove has two separate chambers, one serves as the combustion chamber, and the other serves as the pyrolysis chamber. In order to maximize contact between two chambers and transfer as much heat from combustion to biomass as possible to facilitate pyrolysis reaction, Cook-Stove is designed to be two concentric cylinders with combustion chamber inside and pyrolysis chamber outside.



*Figure 1.1: Real Cook-Stove structure*

For pyrolysis purpose, biomass- left over from crops and forests -is chosen to perform this role for its accessibility and affordability. While being pyrolyzed, biomass generates considerable amount of heat and produces char as one of its major by-products, which is beneficial to soil and, therefore, welcomed by farmers. Common open Cook-Stove, on the other hand, creates large amount of smoke, CO and pollution as it operates.



*Figure 1.2: Loading the pyrolysis chamber with corn cobs*

Over 30 pyrolysis Cook-Stoves designed by Cornell students are currently working in Kenya. While actual data is being collected from our stoves, we would also like to have a better understanding of its internal dynamics and, ultimately, develop some design ideas.



*Figure 1.3: Pyrolysis Cook-Stoves used in Kenya*

While fuel is combusting rather thoroughly in the combustion chamber, there is still leftover biomass present in the pyrolysis chamber, which means that there is still room for improvement. Moreover, the amount of biomass pyrolyzed is directly proportional to the amount of energy it produces. Therefore, our simulation will focus on the modeling of pyrolysis chamber.

Our report will cover the development of ANSYS Fluent model, model verification and optimization.

The purpose of this report is to introduce a model that can simulate the heat transfer process inside the pyrolysis chamber, and to propose several optimization ideas that can improve its performance. Afterwards, the report will include discussion and analysis of the results of our optimization ideas that are evaluated using model predictions. Finally, some recommendations will be included to help future research.

## 2 Development of Model

In this chapter, the process of model development will be introduced. ANSYS will be used to creating geometry, generating mesh and modeling. In particular, ANSYS Fluent will be used to simulate the heat transfer and chemical reaction inside the pyrolysis chamber.

ANSYS offers engineering simulation solution sets in engineering simulation that a design process requires. ANSYS Fluent is an ideal computational fluid dynamic simulation software that models heat transfer and reactions.

To build an ANSYS model, first, the original complicated pyrolysis chamber structure needs to be simplified. Then the simplified geometry will be drawn in the ANSYS Design Modeler and mesh will be generated in ANSYS Meshing. After that, the mesh will be imported into FLUET and boundary conditions will be set up. Finally, a program that can represent the pyrolysis reaction will be implemented by User Defined Function.

The sequence of this chapter will follow the procedures described above.

### 2.1 Simplification to 2-D Axisymmetric Geometry

The geometry of the Cook-Stove is complicated and hard to model (Figure 1.1, Figure 1.3). Thus a simplification is necessary.

The first step is to convert the complicated geometry to a simplified 3-D geometry. The Cook-Stove consists of three concentric annular chambers. The inner annulus is the combustion chamber where fuel reacts to provide heat for both cooking and pyrolysis reaction. The middle annulus is the pyrolysis chamber where char and gas are generated via pyrolysis. These two chambers share a wall while the outer wall of the pyrolysis chamber is slightly higher than the wall between pyrolysis and combustion chamber which will be simplified to the same height. The outer annulus exists for safety purposes. After filling the pyrolysis chamber with biomass, a lid will cover those chambers and that lid can support the pot. Instead of sealing the pyrolysis chamber from combustion chamber, an opening exists between those two chambers so that char and other gases can flow from pyrolysis chamber to the combustion chamber. We can call this opening the outlet, this outlet will be placed in the inner wall of the pyrolysis chamber. On the other hand, there is a wood feed channel though the convection chamber and the pyrolysis chamber which will be neglected in the simplified model.

Since the pyrolysis chamber is the chamber to model, it is separated from the whole structure of the Cook-Stove. The pyrolysis chamber is simplified as annulus that has a height of 0.2m with inner radius of 0.09m, outer radius of 0.14m and outlet width of 0.008m (Figure 2.1).

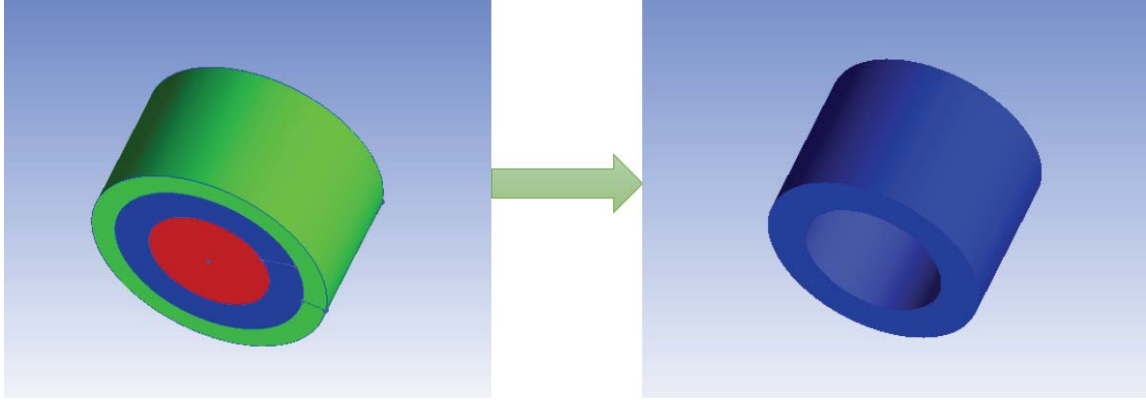


Figure 2.1: Simplified pyrolysis chamber

The boundary condition is independent of angular position at the inner wall of the pyrolysis chamber which is connected to the combustion chamber. Also, the boundary at the chamber outer wall is independent of angular position. As a result, aiming to improve computational efficiency, only a two dimensional slice is needed for our simulation, as shown in figure 2.2.

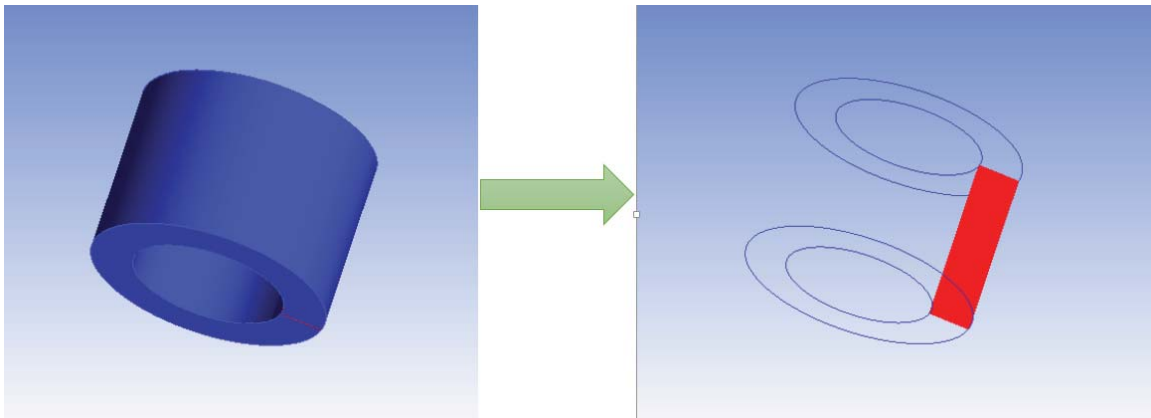


Figure 2.2: 3D to 2D simplification

Figure 2.3 shows the final simplified geometry with name selections.

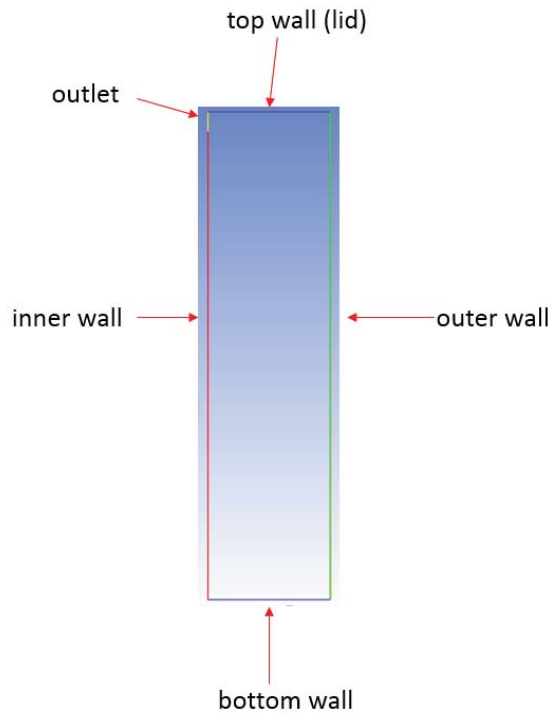


Figure 2.3: Simplified 2D model

## 2.2 Geometry

After model simplification, we started to pivot our attention to the boundaries that surround our pyrolysis chamber – chamber walls. First, we investigated the heat capacity of chamber walls, since they are made of iron that has a relatively high density compared to biomass. Their heat capacity implies that the amount of heat stored in chamber walls should effectively slow heating process down. Moreover, iron also has greater conductivity than biomass; heat should travel faster in iron than in biomass. After a certain amount of time, as the bottom chamber wall becomes hotter than the biomass, the stove essentially have more heating surface than designed.

Prior to including chamber walls into our model, we would like to confirm how significant an impact we should experience once chamber walls are included. In order to do that, a calculation was conducted to validate our concerns about the chamber walls. Essentially, the product of mass and its heat capacity will tell us the heat storage significance of chamber walls, and as for larger heating surface, we will have to observe that in actual simulation.

We compute the heat capacity of each material from its specific heat, volume and density:

$$M_i * C_i = V_i \rho_i C_i$$

with  $M_i$  stands for mass,

$V_i$  stands for volume,

$\rho_i$  stands for density,

$C_i$  stands for specific heat capacity.

Table 2.1 shows individual specific heat, density, volume and heat storage of every part. As can be seen, the amount of heat can be stored in metal is approximately the same as biomass.

$$\frac{M_m C_m}{M_w C_w} = \frac{2332.4 + 629.7}{2926.4} = 1.01$$

with  $M_m C_m$  stands for the heat storage of metal,

$M_w C_w$  stands for the heat storage of biomass.

As a result, all four of chamber walls should be taken into consideration when we build our model using ANSYS Model Designer (Figure 2.4).

Table 2.1: Chamber wall calculation result

	Inner & outer walls	Top & bottom walls	Biomass in the pyrolysis chamber
$C_i$ (J/kg/K)	502.48	502.48	1500
Density (kg/m <sup>3</sup> )	8030	8030	450
Volume (m <sup>3</sup> )	5.78E-04	1.56E-04	7.22E-03
$M_m * C_m$ (J/K)	2332.4	629.7	2926.4

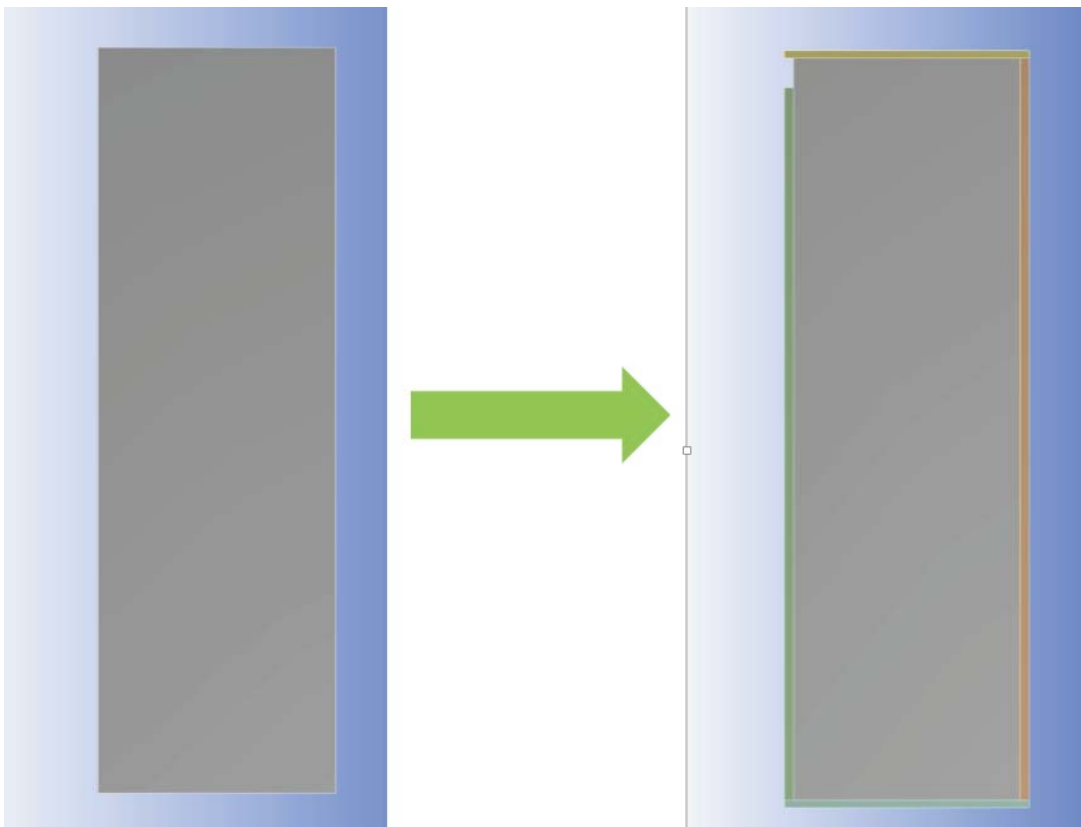


Figure 2.4: 2D geometry with chamber wall



## 2.3 Mesh

On the one hand, the quality of mesh can influence the accuracy of the simulation result. On the other hand, the total number of cells and nodes affects the simulation time. The metric of a good mesh is to acquire an accurate result in relatively short time.

In the process of generating a mesh for the model, a uniform mesh was tried, and then replaced by a refined mesh which has much higher accuracy without much cell number increase.

### 2.3.1 Uniform Mesh

Mesh is generated using ANSYS Meshing. Considering that we are going to use FLUENT to simulate an axisymmetric model, and the valid symmetric axis in FLUENT is the x axis, the model will be rotated 90 degrees counterclockwise.

Since the outline of geometry is approximately a rectangle, mesh that is generated in a uniform fashion should have a high mesh quality. Under the guidance of this principle, all cells are generated in the same length and width, which is one millimeter (Figure 2.5). The total number of cells is 11000.

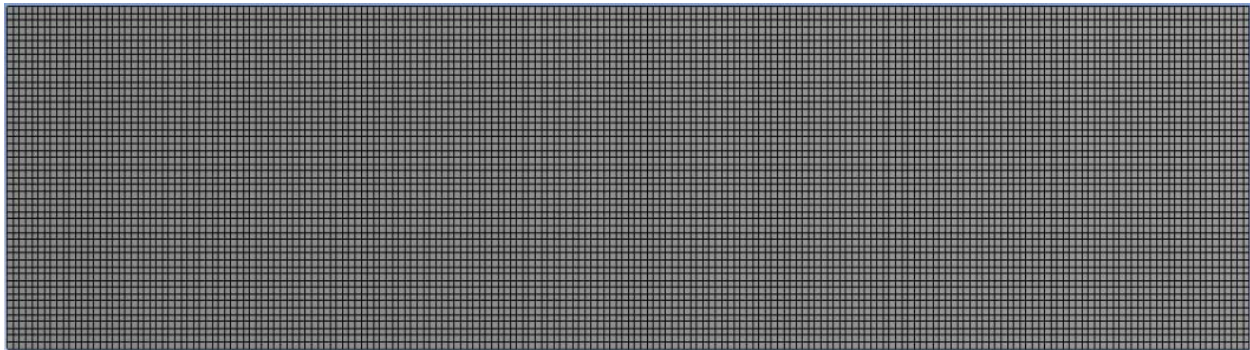


Figure 2.5: Uniform mesh

### 2.3.2 Refined Mesh

As shown in Figure 2.6, the heat flux will mainly flow along the y direction due to the position of combustion chamber. The temperature gradient along x direction will be much lower than that in the y direction, which means that the cell length in the x direction can be increased to decrease the cell number and the cell length in y direction should be compressed to acquire better accuracy. Considering the boundary layer effect near the wall, compressed cells are used near the combustion wall and the convection wall.

Consequently, the cells shift from perfect quadrates to quasi-rectangles, while mesh quality suffers little. The orthogonal quality after refinement is 0.94 compared to that of 0.99 before refinement. With a range of 0 to 1, any quality above 0.4 is considered acceptable.

With an acceptable sacrifice of mesh quality, the refined mesh can perform more accurate simulations without increasing the simulation time too much. The total cell number for the refined mesh is 17760.

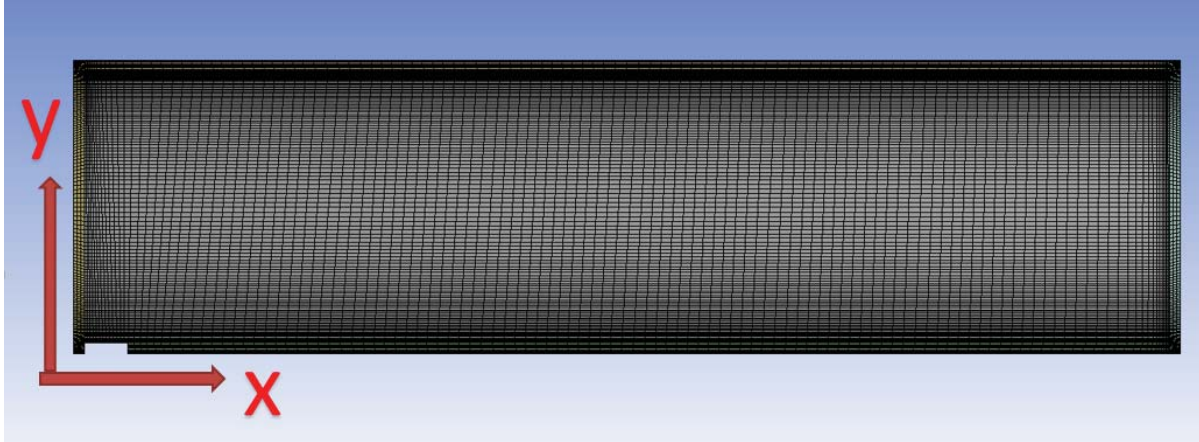


Figure 2.6: Refined mesh

The refined mesh (Figure 2.6) will be used in the following analysis. Section 3.1 will further investigate the effect of cell size to the results.

## 2.4 Material Properties and Boundary Conditions

After geometry building and mesh generation, the mathematical model needs to be set up in FLUENT.

In ‘General’, solver type is Pressure-Based; simulation time is set to be transient; velocity formulation is set to be absolute and due to the simplification method, this is a 2D rotational axisymmetric simulation. For the completeness of the simulation, gravity is activated and a  $9.81 \text{ m/s}^2$  gravitational acceleration is added to the x direction because the symmetric axis is x axis as stated in section 2.3.1.

In ‘Models’, since for now heat transfer is the only model considered, ‘energy’ is switched on and ‘viscous option’ is laminar.

In ‘Materials’, since we are simplifying the model, methane will be assigned to represent all the pyrolysis gases in the pyrolysis chamber. There are three kinds of materials that are needed for the model. Methane and biomass are inside of the pyrolysis chamber, while the chamber wall is steel. Table 2.2 (ToolBox, 2014) (ToolBox, Gases - Specific Heats and Individual Gas Constants, 2014) shows the properties of different materials.

Table 2.2: Material properties

Material	Density ( $\text{kg/m}^3$ )	Cp (J/kg*K)	Thermal Conductivity (W/(m*K))
Methane	0.067	piecewise-polynomial	0.0332
Steel	8030	502.48	16.27
Biomass	450	1500	0.17

In ‘Cell Zone Conditions’, five domains are present in this model. Four of them are chamber walls and the other one is the area inside the chamber. For better simulation of the heat transfer inside the pyrolysis

chamber, biomass and methane inside the chamber can be treated as a porous medium in which heat can be either conducted through the biomass or transferred by convection through the methane. Therefore, within the porous medium, the fluid material is methane and the solid material is biomass. Porosity is set to be 0.4 (Chen, 2011) and thermal model is equilibrium model. As for the other four chamber wall domains, all of them should be steels and none source term is needed.

In 'Boundary Conditions', there are several boundary parameters require close attention.

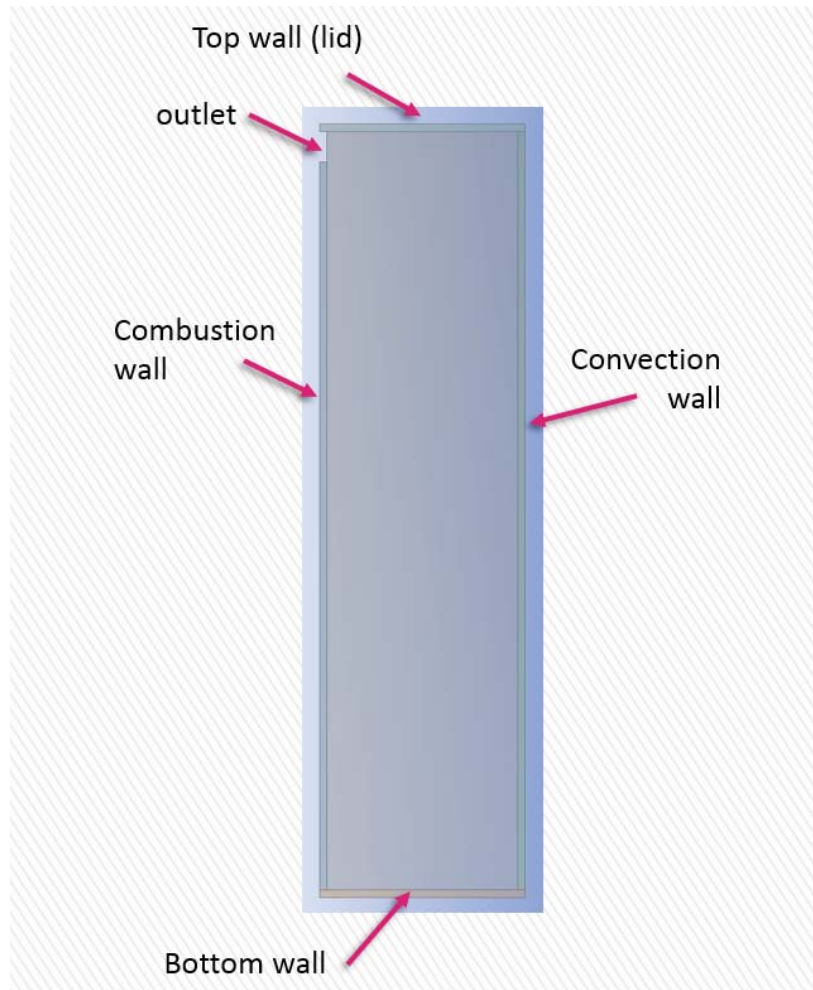


Figure 2.7: Name selections for different boundaries

Combustion wall is the interface between the combustion chamber and the pyrolysis chamber, where heat generated by combustion is conducted to biomass and methane. So the heat transfer coefficient is estimated at  $100 \text{ W}/(\text{m}^2 \text{ K})$  and the free stream temperature is  $1000\text{K}$ .

Convection wall is the interface between the pyrolysis chamber and the convection chamber. A certain amount of heat coming from the combustion and pyrolysis reaction is dissipated through this wall. So the heat transfer coefficient is estimated at  $20 \text{ W}/(\text{m}^2 \text{ K})$  and the free stream temperature is  $300\text{K}$ . This heat transfer coefficient is different from the combustion wall because heat transfer near combustion is much stronger than natural convection due to the turbulence generated by the flame.

The Outlet should be a pressure-based boundary condition that has the same parameters as the combustion chamber, which is 1000K and 1atm.

In Fluent, boundary conditions are automatically symmetrical if not changed, so both top wall and bottom wall are automatically set to be adiabatic boundary conditions.

In ‘Monitors’, the monitor checks convergence absolute criteria for continuity, x-velocity, y-velocity and swirl should be 1E-5 to ensure accuracy.

In ‘Solution Initialization’, the initial temperature is 300K as the ambient temperature

The rest of the settings should remain default.

Table 2.3: Boundary conditions

Boundary	Mode	Heat transfer coefficient (W/(m <sup>2</sup> *K))	Free stream temperature (K)
Combustion wall	convection	100	1000
Convection wall	convection	20	300
Outlet	pressure-outlet	N/A	1000
Top wall	adiabatic	N/A	N/A
Bottom wall	adiabatic	N/A	N/A

Table 2.3 shows the estimated boundary conditions that will be adjusted by comparing with experimental results later when the model is built.

## 2.5 Heat Source (Chemical Reaction)

With all settings confirmed, adding the pyrolysis process to the model became the highest priority. Since chemical reactions are not one of FLUENT’s strong suits, User-defined function (UDF) should serve as the approach to implement the reactions and heat source should serve as the implementation of the reactions. Programming C is the only language recognized by FLUENT, therefore, we would also be using MS Visual Studio.

We started with the simplest model, which is merely a uniform heat source that is independent of time, temperature and remaining reactants. Afterwards, with one step at a time, we added time dependence and local temperature dependence into our heat source. Finally, with the mass fraction of remaining reactants present, our heat source is feasible within the scope of this project.

### 2.5.1 Uniform Heat Source

Using the reaction mechanism shown in figure 2.8, the heat of reaction is the sum of products of individual reaction heat release and their corresponding weight percentage. Using typical data for this type of reactions (Teeranai Pattanotai, 2014), tar and gas constitute 65% and 15% respectively, with  $\Delta H$  of -80 kJ/kg, while 20% of char has a  $\Delta H$  of 220 kJ/kg.

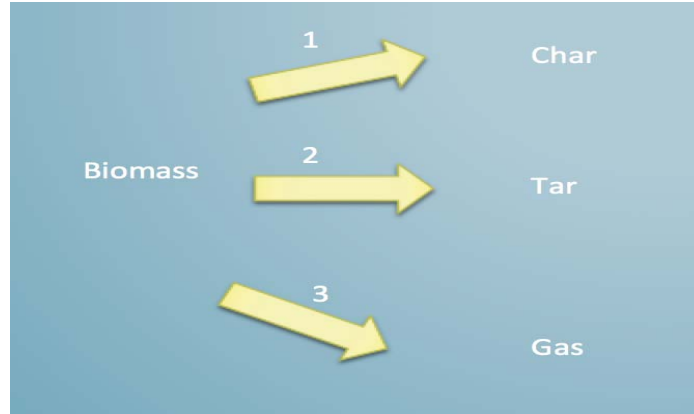


Figure 2.8: Reaction mechanism

The amount of heat released per volume is heat of reaction per mass times density of reactant times porosity of reactants over time duration.

Calculation:

$$\Delta H = 220 \frac{\text{kJ}}{\text{kg char}} * 0.2 \frac{\text{kg char}}{\text{kg biomass}} + (-80) \frac{\text{kJ}}{\text{kg tar or gas}} * (0.65 \frac{\text{kg tar}}{\text{kg biomass}} + 0.15 \frac{\text{kg gas}}{\text{kg biomass}})$$

$$= -20 \text{ kJ/kg}$$

$$Q = -20 * 450 * 0.6 * 1000/1800$$

$$= -3000 \text{ W/m}^3$$

Since this is a uniform endothermic heat source, no UDF is needed; Heat source can be implemented directly in FLUENT.

## 2.5.2 Time Dependent Heat Source

After successfully implementing uniform heat source, more details are required to improve our heat source interpretation. As endothermic and exothermic reactions are not simultaneous in nature, time dependence of each reaction should be included.

### 2.5.2.1 Calculation

With the help and data from Professor Fisher, it has been determined that:

In the first 10 minutes, no reaction available;

From 10 to 25 minutes, endothermic reaction is in;

From 25 to 40 minutes, both reactions are in;

From 40 to 55 minutes, exothermic reaction is in.

The amount of heat released per volume is heat of reaction per mass times density of reactant times porosity of reactants over time duration.

Endothermic reaction:

$$Q = -80 \frac{\text{kJ}}{\text{kg tar}} * 1000 \frac{\text{j}}{\text{kg}} * 0.8 \frac{\text{kg tar/gas}}{\text{kg biomass}} * 450 \frac{\text{kg}}{\text{m}^3} * 0.6 \frac{\text{m}^3 \text{ biomass}}{\text{m}^3 \text{ chamber}} / 1800 \text{ second}$$

$$= -9600 \text{ W/m}^3$$

Exothermic reaction:

$$Q = 220 \frac{\text{kJ}}{\text{kg char}} * 1000 \frac{\text{j}}{\text{kg}} * 0.2 \frac{\text{kg char}}{\text{kg biomass}} * 450 \frac{\text{kg}}{\text{m}^3} * 0.6 \frac{\text{m}^3 \text{ biomass}}{\text{m}^3 \text{ chamber}} / 1800 \text{ second}$$

$$= 6600 \text{ W/m}^3$$

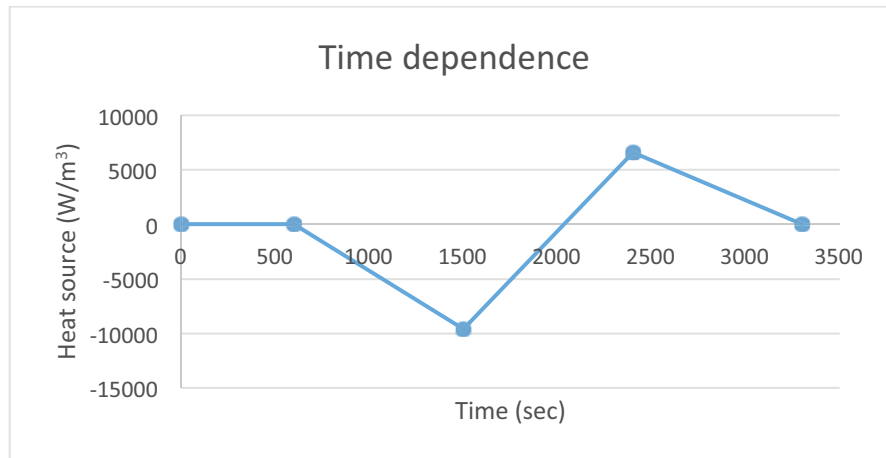


Figure 2.9: Reaction plot

Combinations of both endothermic and exothermic reactions are shown in figure 2.9.

Combinations:

$$Q = 0 \text{ W/m}^3 \quad 0 < t < 600, t > 3300$$

$$Q = -\frac{32}{3} * (t - 600) \text{ W/m}^3 \quad 600 < t < 1500$$

$$Q = 18 * t - 36600 \text{ W/m}^3 \quad 1500 < t < 2400$$

$$Q = -\frac{22}{3} * (t - 3300) \text{ W/m}^3 \quad 2400 < t < 3300$$

### 2.5.2.2 Code

Figure 2.10 shows the actual code.

```

/*****
UDF for time dependent volumetric heat generation of cell
*****/
#include "udf.h"
#define C1 -10.666//define constant term
#define C2 6400
#define C3 18
#define C4 -36600
#define C5 -7.333
#define C6 24200

DEFINE_SOURCE(heat,cell,thread,dS,eqn)
{
    real source;
    real time;
    time = CURRENT_TIME; //taking time value;

    if (time < 600)
    {
        source = 0;//time dependent heat source;
        dS[eqn] = 0;
    }
    else if (time >= 600 && time < 1500)
    {
        source = C1*time+C2;
        dS[eqn] = 0;
    }
    else if (time >= 1500 && time < 2400)
    {
        source = C3*time+C4;
        dS[eqn] = 0;
    }
    else if (time >= 2400 && time < 3300)
    {
        source = C5*time+C6;
        dS[eqn] = 0;
    }
    else
    {
        source=0;
        dS[eqn] = 0;
    }
    return source;
}

```

Figure 2.10: Time dependent heat source

### 2.5.3 Local Temperature Dependent Heat Source

Upon successfully implementing a time-dependent heat source in the code, dependence on both local temperature and remaining mass fraction of reactant is left to improve our UDF heat source code. Therefore, we switch to local temperature dependence to further our project.

#### 2.5.2.1 Calculation

Based on the relationship between local temperature and heat release obtained from papers and documents (Teeranai Pattanotai, 2014), we now have this:

The amount of heat released per volume is the heat of reaction per mass times density of reactant times porosity of reactants times coefficient of local temperature.

$$Q = -20 \frac{\text{kJ}}{\text{kg biomass}} * 1000 \frac{\text{j}}{\text{kg}} * 450 \frac{\text{kg}}{\text{m}^3} * 0.6 \frac{\text{m}^3 \text{ biomass}}{\text{m}^3 \text{ chamber}} * 1.08e10 * \exp\left(-\frac{148000 \frac{\text{J}}{\text{mole}}}{8.314 \frac{\text{J}}{\text{mole K}} * T \text{ K}}\right)$$

$$= -2.3328e17 * \exp(-17801.3/T) \text{ W/m}^3$$

### 2.5.2.2 Code

Figure 2.11 shows the actual code

```

/*****
UDF for time dependent volumetric heat generation of 18650 cell
*****/
#include "udf.h"
#define C1 -2.332//define constant term
#define C2 100000
#define C3 100000
#define C4 100000
#define C5 100
#define C6 -17801.3

DEFINE_SOURCE(heat_teperature,cell,thread,dS,eqn) //DEFINE_SOURCE(heat_haolun,cell,thread,dS,eqn)
{
double source;

real temp = C_T(cell, thread);

source = C1*C2*C3*C4*C5* exp (C6/temp) ;
dS[eqn] = 0;
return source;
}

```

Figure 2.11 Temperature dependent heat source

### 2.5.4 Local Temperature and Mass Fraction Dependent Heat Source (Char Formation)

Finally, we include remaining mass fraction of reactant dependence to make our simulation more realistic, since mass fraction of reactant as well as temperature are major factors in how fast the reaction goes.



### 2.5.4.1 Calculation

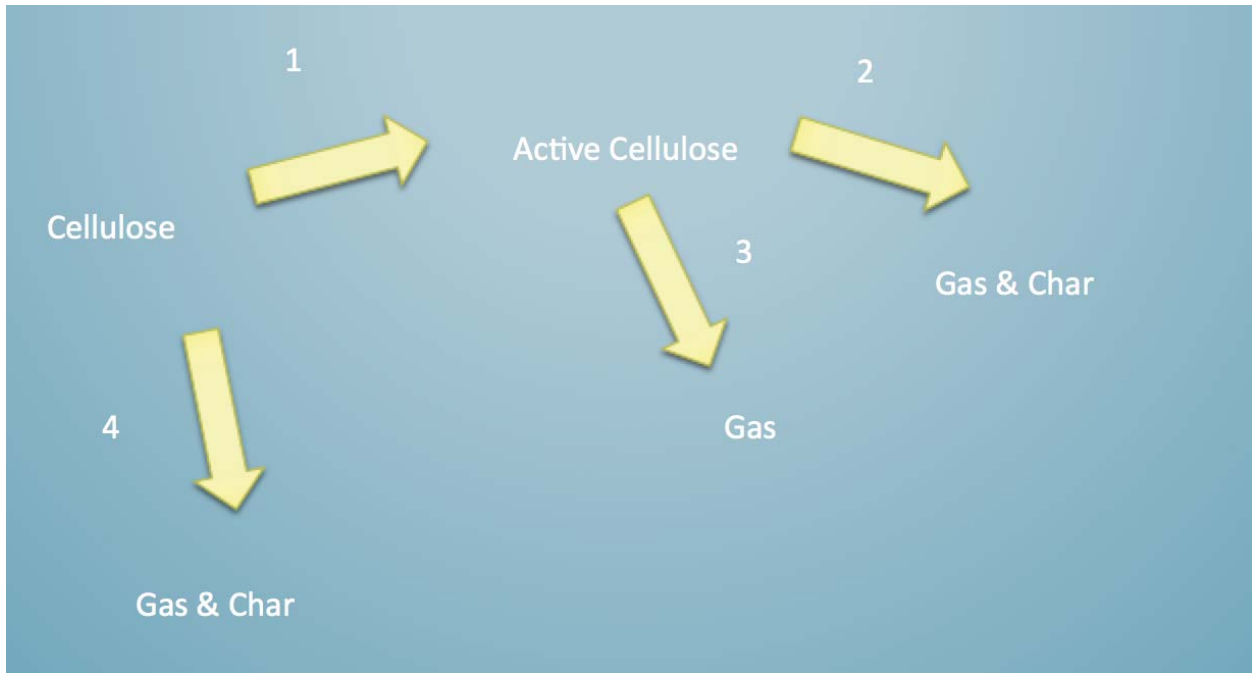


Figure 2.12: Reaction mechanism

In reality, biomass is composed of many components. Cellulose is the largest of the components present in biomass, which is why we chose to model with just biomass. Given our temperature range is below 800 K, cellulose is our initial reactant as shown in figure 2.12, and it branches into two reactions, one of which generates active cellulose and the other generates gas and char. Once active cellulose is generated, it also branches into two reactions, which give us gas and char as products.

Table 2.4: Reaction parameters (Teeranai Pattanotai, 2014)

	EA	A	Heat of reaction (kJ/kg)
Reaction 1	-188400	4.00E+13	0
Reaction 2	-80000	2.00E+06	-109500
Reaction 3	-41860	4*Temperature	-100900
Reaction 4	-129800	6.50E+07	268000

As shown in table 2.4, we have all the parameters we needed to complete our code, from reaction rate parameters to heat of reaction.

The formulas we used are describing a first order reaction with Arrhenius kinetics. Here we show an example set of equations for reaction 1.

$$\frac{dy_B}{dt} = -k(T) * y_B$$

$$Q = \Delta H * k(T) * y_B * \rho_B * p \text{ (W/m}^3\text{)}$$

$$k(T) = A * \exp\left(\frac{-EA}{RT}\right)$$

With  $y_B$  stands for mass fraction of cellulose,

$k(T)$  stands for reaction rate,

$\Delta H$  stands for heat of reaction,

$p$  stands for porosity of reactant,

$\rho_B$  stands for density of cellulose.

The amount of heat released per volume is the heat of reaction per mass times density of reactant times porosity of reactant times coefficient of local temperature times mass fraction of cellulose.

#### 2.5.4.2 Code

Figure 2.13 shows the actual code

```
#include "udf.h"

DEFINE_INIT(init_UDMI, domain)
{
    cell_t c; /* Cell index has its own type too */
    Thread *ct; /* Threads are pointers to a structure */

    thread_loop_c(ct,domain)
    {
        begin_c_loop(c,ct) /* Loop through all the cell threads in the domain */
        /* Loop through the cells in each cell thread */
        {
            C_UDMI(c,ct,0) = 1.0; /*cellulose mass fraction, initialize it as 1.0*/
            C_UDMI(c,ct,1) = 0.0; /*active cellulose mass fraction, initialize it as 0.0*/
            C_UDMI(c,ct,2) = 0.0; /*char mass fraction, initialize it as 0.0*/
            C_UDMI(c,ct,5) = 0.0; /*heat source, initialize it as 0.0*/
        }
        end_c_loop(c,ct)
    }
}

DEFINE_EXECUTE_AT_END(execute_at_end)
{
    double deltaxone;
    double deltaxtwo;
    double deltaxthree;
    double deltaxfour;
    double sourcetwo;
    double sourcethree;
    double sourcefour;

    Domain *domain = Get_Domain(1); /*need to get the domain pointer because it is not passed as an argument by thus UDF*/
    cell_t cell;
    Thread *thread;
    real temp; /*cell and thread needs to be defined in order to use them*/

    real dt = CURRENT_TIMESTEP; /*CURRENT_TIMESTEP can get the current time step size*/

    thread_loop_c(thread,domain)
    {
        begin_c_loop(cell,thread)
        {
            temp = C_T(cell, thread);

            deltaxone = 0.0;|
            deltaxtwo = 0.0;
            deltaxthree = 0.0;
            deltaxfour = 0.0;
        }
    }
}
```

```

if (C_UDMI(cell,thread,0) > 0 )
{
    deltaxone=exp(-22660.57/temp)*(4.0e+13);          /*time difference is set to be 1 second; -- use dt instead of 1*/
    deltaxfour=exp(-15612.22/temp)*(6.5e+7);

}

C_UDMI(cell,thread,0)+= C_UDMI(cell,thread,0)*(-deltaxone-deltaxfour)*dt;
C_UDMI(cell,thread,0) = MAX(C_UDMI(cell,thread,0), 0.0);
C_UDMI(cell,thread,1)+= C_UDMI(cell,thread,0)*deltaxone*dt;

if (C_UDMI(cell,thread,1) >= 0)
{
    deltaxtwo=exp(-9622.323/temp)*(2.0e+6);
    deltaxthree=exp(-5034.88/temp)*(4)*temp;

}

C_UDMI(cell,thread,1)+= C_UDMI(cell,thread,1)*(-deltaxtwo-deltaxthree)*dt;
C_UDMI(cell,thread,2)+= C_UDMI(cell,thread,1)*(0.045*deltaxtwo+0.444*deltaxfour+0*deltaxthree)*dt;
C_UDMI(cell,thread,1) = MAX(C_UDMI(cell,thread,1), 0.0);
C_UDMI(cell,thread,2) = MAX(C_UDMI(cell,thread,2), 0.0);

sourcetwo=270/0.162*deltaxtwo*(-1.095e+5)*C_UDMI(cell,thread,1);
sourcethree=270/0.162*deltaxthree*(-1.009e+5)*C_UDMI(cell,thread,1);
sourcefour=270/0.162*deltaxfour*(2.68e+5)*C_UDMI(cell,thread,0);
C_UDMI(cell,thread,5) =sourcetwo+sourcethree+sourcefour;          /*Heat source, Make sure a has unit of W/m^3*/
}
end_c_loop(cell,thread)
}
}

/*DEFINE_SOURCE(heat_temperature,cell,thread,dS,eqn)*/
DEFINE_SOURCE(heat_temperature,cell,thread,dS,eqn)
{
    double source;

    source = C_UDMI(cell,thread,5);
    dS[eqn] = 0;
    return source;
}

```

Figure 2.13: Mass fraction and temperature dependent heat source

### 2.5.5 Future Coding Direction

As mentioned before, our code is as complete as our schedule permits, which means there still is room for improvements for future students.

First of all, we merely considered cellulose as reactant and ignored other less reactive or less weighted components within biomass. Based on same coding structure, multiple reactants should be easily implemented.

Moreover, the nature of gas indicates it would generate pressure difference between pyrolysis chamber and combustion chamber, which would cause a flow from the pyrolysis chamber through the outlet into the combustion chamber. Once gas starts to ventilate, it transfers heat along with itself. Therefore, even though we included gas as part of our products, we failed to take convection into consideration. Changing from natural convection to forced convection within pyrolysis chamber should influence heat transfer significantly.

### 3 Simulation Results and verification

Chapter 2 introduced the development of the model. While most of the parameters in the model are acquired from actual data and measurement, there still exist some parameters that are based on estimation. So some verification of results needed before we proceed with the design.

In this chapter, three different ways to verify and to improve the model are introduced. First, mesh sensitivity will be checked to eliminate the influence of different mesh on the simulation result. Second, some estimated parameters will be selected by comparing simulation results to the experimental data. Third, the heat source added in the final model will be verified by calculation.

#### 3.1 Mesh sensitivity check

The purpose of mesh sensitivity check is to confirm that the simulation result is not sensitive to the cell number so that even though cell number were increased by a large fraction, the simulation result can still remain similar.

In order to check mesh sensitivity, three different meshes are simulated. The number of cells is altered for every simulation while boundary conditions remains the same. Mass fractions of unreacted cellulose of each simulation at 4000s and 7500s (these two times are characteristic simulation times for this model, will be introduced in the following sector) are measured and compared.

Figure 2.6 shows the original mesh, Figure 3.1 and Figure 3.2 shows the new meshes generated for comparison.

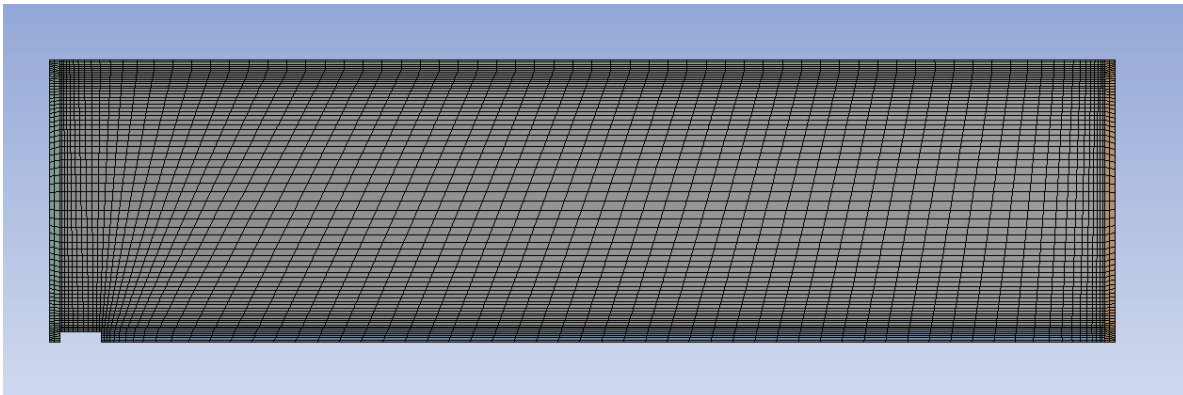


*Figure3.1: Mesh 1 (5195 cells)*

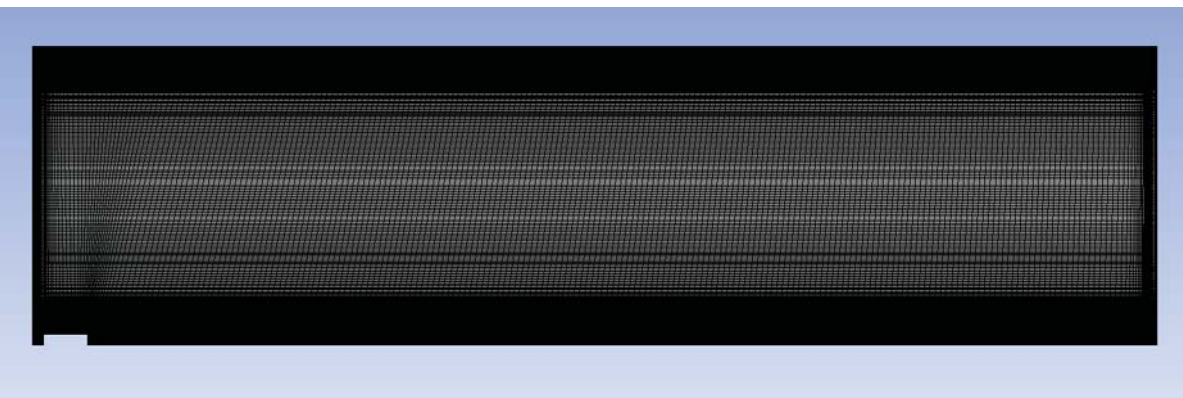


*Figure 3.2: Mesh 2 (70120 cells)*

Table 3.1: Mesh sensitivity check result

Mesh type	Number of cells	Remaining cellulose	
		4000s	7500s
Reference mesh	17760	38.93%	33.86%
mesh 1	5195	36.91%	31.62%
mesh 2	70120	38.89%	33.77%

As the result shown in table 3.1, number of cells in mesh 1 is only 30% of the reference mesh, while number of cells in mesh 3 is four times as the reference mesh. Relative change of remaining cellulose of mesh 1 at 7500s is 6.6% and relative change of remaining cellulose of mesh 2 at 7500s is 0.27%.

From the result we can see that the reference mesh is refined enough, because compare to the result of mesh 2, which is obviously more accurate because of higher number of cells, the result of mesh 1 is significantly more different than that of reference mesh.

### 3.2 Parameter specification

There are six parameters in current model that are based on estimation: heat transfer coefficient and free stream temperature in convection wall 1 and 2; thermal conductivity of the biomass and simulation time.

To specify the first five parameters, simulation results are compared to the experimental data. One thermocouple was set in the middle of the Cook-Stove and temperature was recorded. After simulation, a temperature monitor point was created in the same location. By changing different values of those five estimated parameters and match them with real situation data, values of parameters are determined.

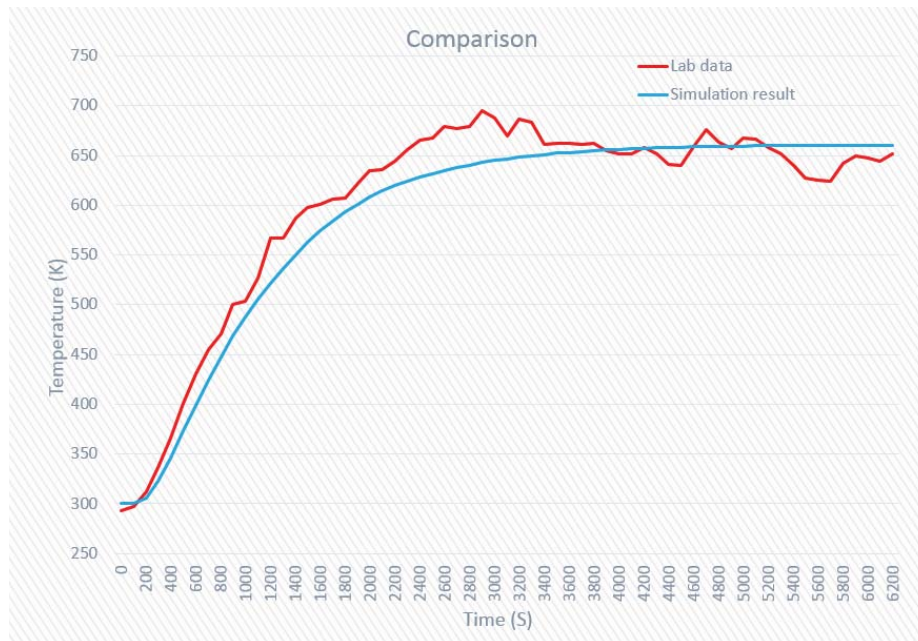


Figure 3.3: Temperature at center of the pyrolysis chamber

Table 3.2 shows the specified parameters.

Table 3.2: Specified parameters

convection wall 1		convection wall 2		thermal conductivity of biomass (W/(m*K))
temperature (K)	heat transfer coefficient (W/(m <sup>2</sup> *K))	temperature (K)	heat transfer coefficient (W/(m <sup>2</sup> *K))	
1000	120	300	20	0.17

Another parameter that need to be specified is the simulation time. Initially, we set up a 20,000 seconds' simulation as the base case, in which the heat transfer reached steady state. According to the result, 71% of cellulose are reacted, we call this percentage base case cellulose mass fraction.

We decided that simulation time should be determined by the time when 90% of the base case cellulose are reacted. After calculation, we found the simulation time is 7500s. Another metric for further evaluating the performance is 4000s, at which 50% of the base case cellulose is reacted.

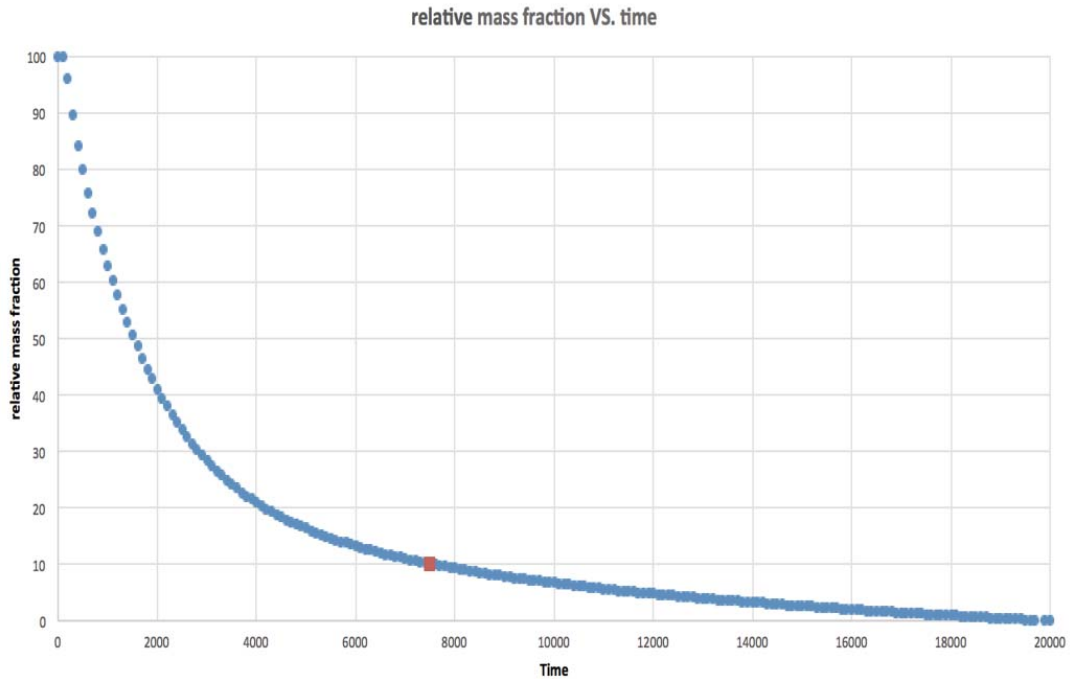


Figure 3.4: Cellulose mass fraction V.S. time

### 3.3 Simulation results

With all the boundary condition and simulation time confirmed (boundary conditions in Table 3.2 and simulation time derived in section 3.2). A complete model was simulated and results are acquired using ANSYS CFD-Post.

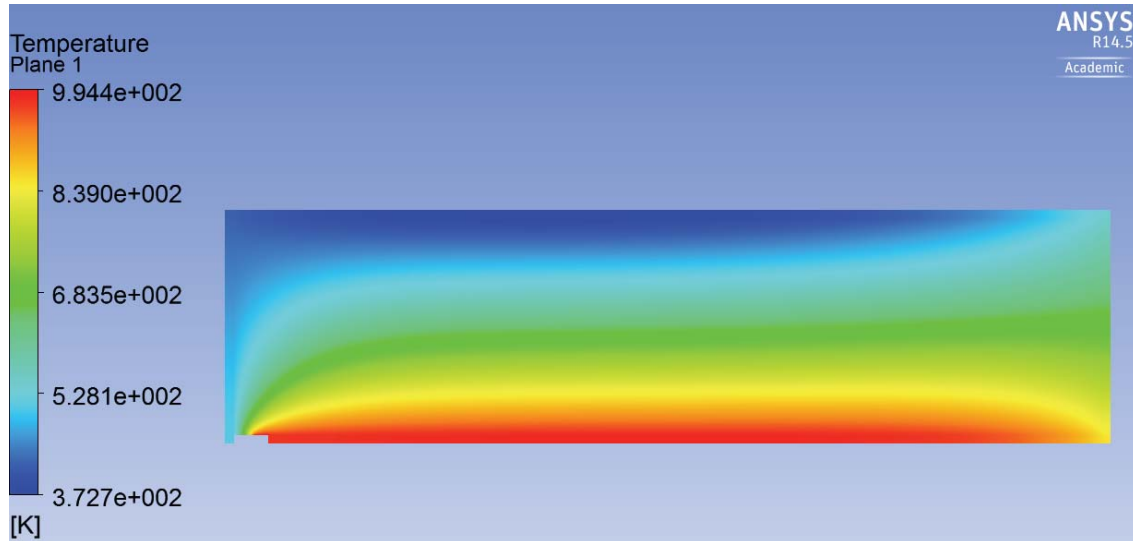


Figure 3.5: Temperature contour at 7500s

Figure 3.5 shows the temperature contour at 7500s. This graph verifies that the temperature gradient in the vertical direction is more significant than that in the horizontal direction.

The average temperature of the porous medium, weighted by area, is 655.2K.

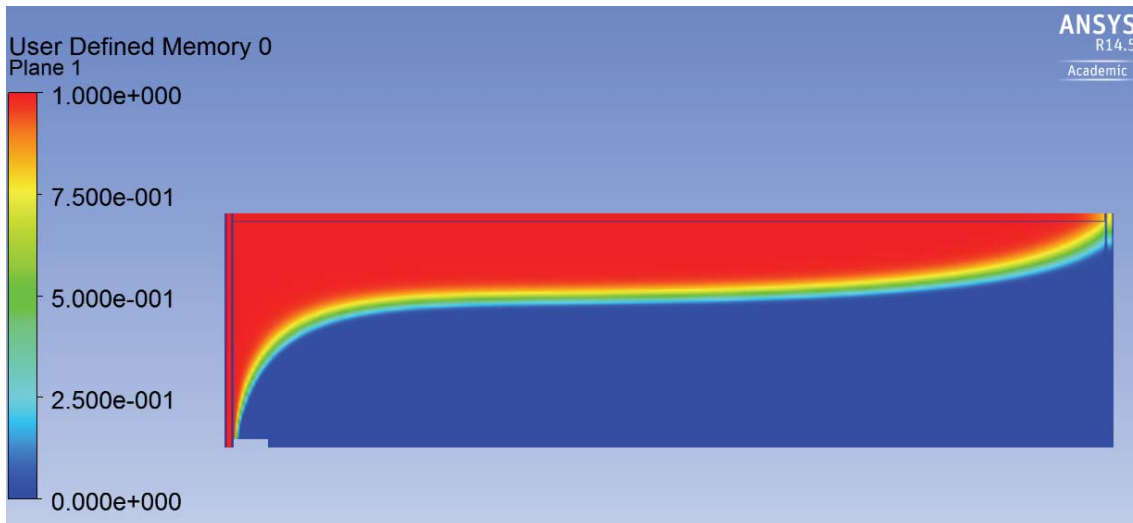


Figure 3.6: Cellulose mass fraction at 7500s

Figure 3.6 shows the cellulose mass fraction at 7500s. At the end of the simulation, about two third of the cellulose are totally reacted (blue part).

The remaining cellulose mass fraction is 33.86%. However, this is an axis symmetric simulation, so the actual remaining cellulose should be calculated by the volume instead of area. The remaining cellulose mass fraction be simplified to:

$$1 - \frac{r_{equivalent} - r_i}{r_o - r_i}$$

Where  $r_{equivalent}$  can be calculated by:

$$r_{equivalent} = r_i + [1 - (2D \text{ mass fraction})] \times (r_o - r_i)$$

In our case,  $r_i = 0.09m$ ,  $r_o = 0.14m$ ,  $(2D \text{ mass fraction}) = 33.86\%$

So the simplified actual remaining cellulose is found to be 38.7%, which means that there is still 38.7% cellulose are not reacted. But for the computational convenience, 2D mass fraction will be used in the future calculation.

### 3.4 Heat Source verification

The heat source means the energy either be generated or absorbed due to the pyrolysis reaction. Since there is no pyrolysis model in FLUENT (as described in section 2.5.4), UDF are used to simulate the chemical reaction.

The pyrolysis reaction that are included in current model is the decomposition of cellulose. This process consists of four reaction. In the first step, cellulose decomposed into active cellulose and gas/char. In the second step, active cellulose further decomposed into char and gas. These reactions and their heat of reactions are already introduced in the previous chapter.

To verify the correctness of the heat source being implemented to the chamber, a back of envelope calculation is performed to find the calculated heat source under the conditions of the simulation; Then these results are compared to the actual heat source that been added in FLUENT.

The first step is to run a simulation of 7500s and acquire data every 100s at four locations. Then, four points are selected to monitor the heat source (Figure 3.7).

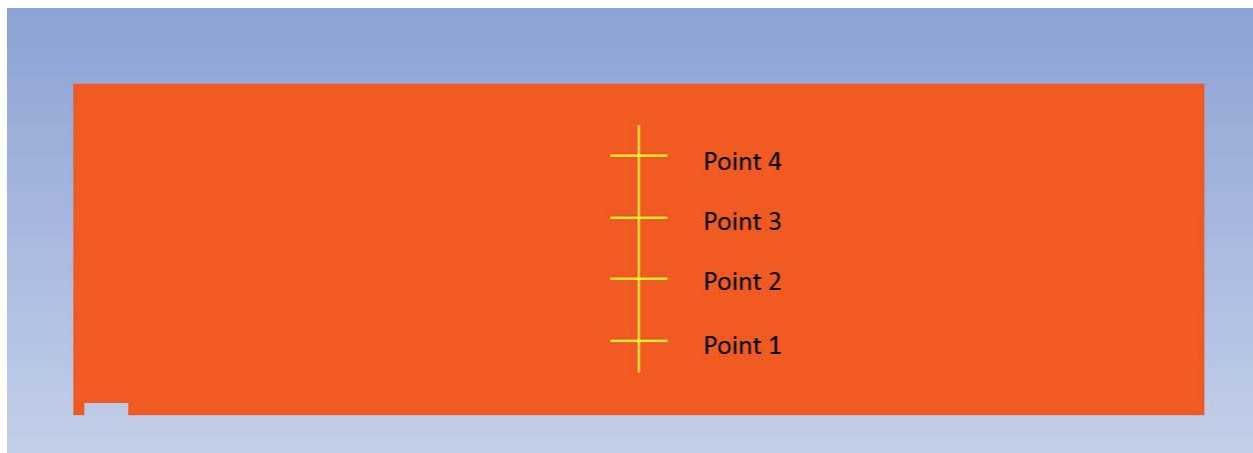


Figure 3.7: Heat source monitor points

The data used is mass fraction of cellulose, active cellulose; temperature and heat source added by FLUENT.



Using the equation introduced in 2.5.4.1, we can find the heat source in four monitor points and compare them with the real heat source implemented by FLUENT. Figure 3.8 to Figure 3.11 show the comparison result.

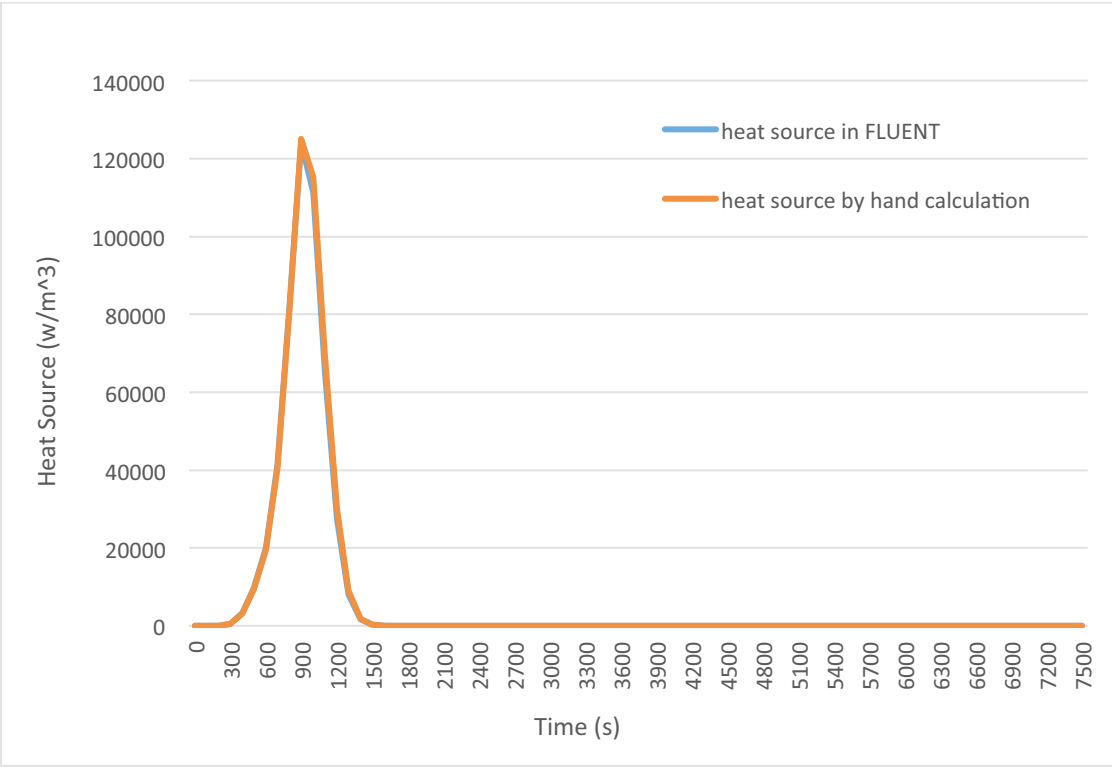


Figure 3.8: Point 1 comparison

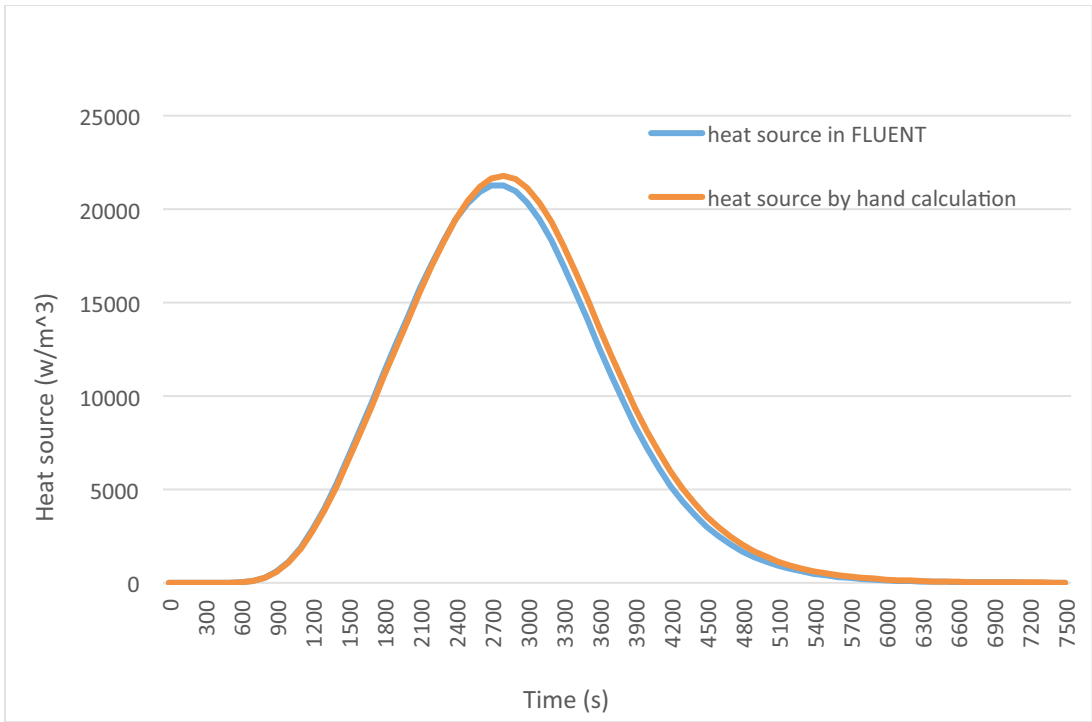


Figure 3.9: Point 2 comparison

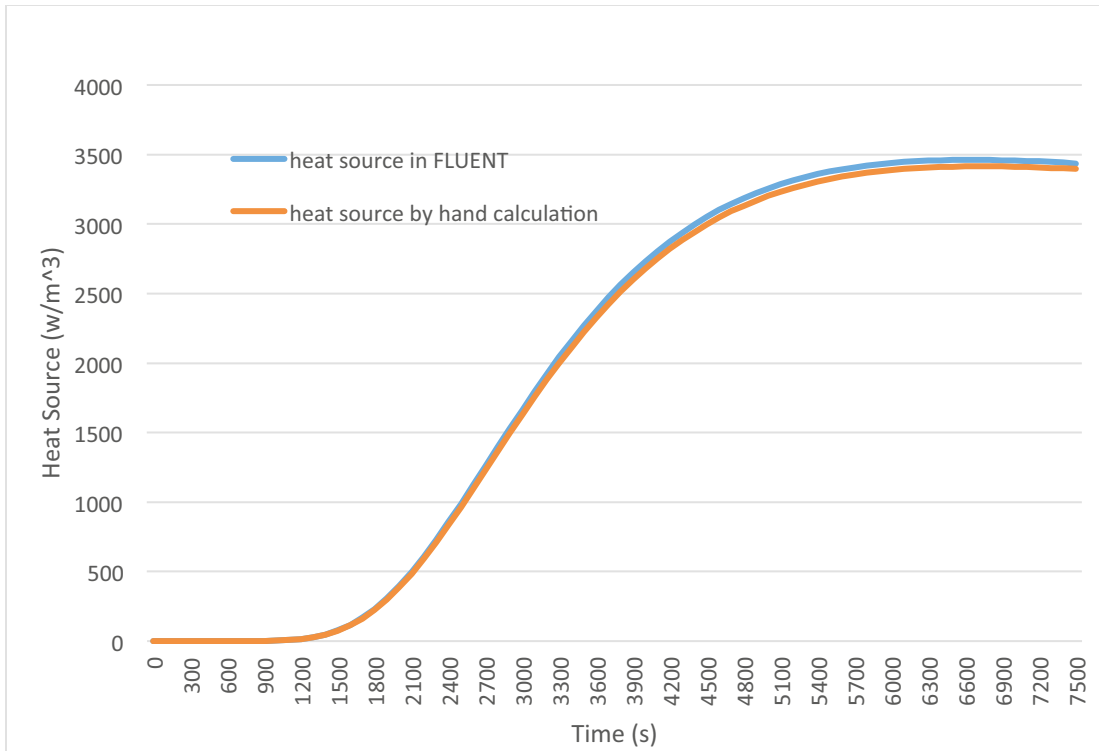


Figure 3.10: Point 3 comparison

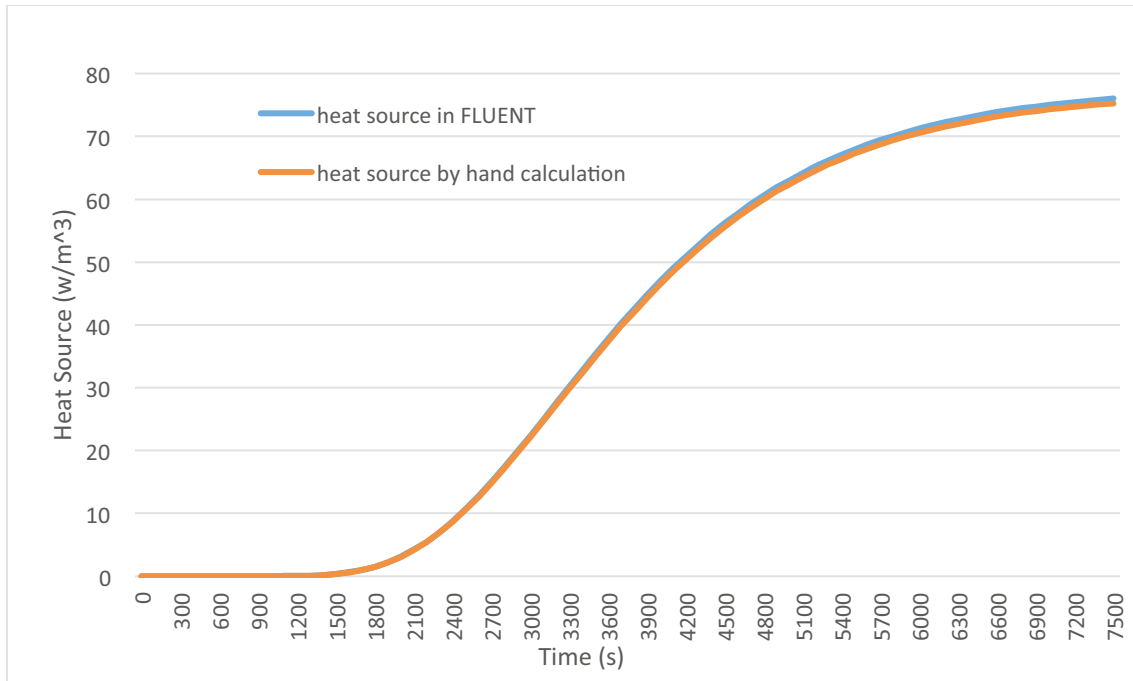


Figure 3.11: Point 4 comparison

According to the result, the two heat sources are perfectly matched. So this result verifies that the heat source added into the model is correct.

## 4 Optimization

In this chapter, design optimization will be introduced. Changes will be made to our stove design one at a time. After simulating in ANSYS Fluent, CFD post-processing will help us to determine Cook-Stove's performance improvement.

First, objectives will be set to evaluate stove design changes. Afterwards, specific optimization ideas will be introduced and discussed. Finally, recommendation will be given based on optimization results.

### 4.1 Objectives

Using the reference set-up validated in Chapter 3, we intend to maximize our biomass conversion as well as shorten the duration to reach quasi steady state.

Table 4.1: Reference set-up and result

Set-up		Remaining cellulose	
Heating wall	Convection wall	4000 s	7500 s
1000K, 120 W/m <sup>2</sup> /K	300K, 20 W/m <sup>2</sup> /K	38.93%	33.86%

Our reference set-up and results are shown in table 4.1. Since the reference set-up is designed to reflect the worst-case scenario, the result should serve as our baseline for any future optimization.

For the following optimization, we will only focus on higher biomass conversion ratio, since higher conversion ratio would correspond to a shorter duration.

## 4.2 Approaches

In this section, we will explore the possible changes we can make to our stove design to improve stove performance, and they are listed as follow:

1. Filling the bottom quarter with materials that have different thermal conductivities.
2. Insulating the convection wall side as well as attaching fins on the heating wall side.
3. Adding heating effect on the lid and contact resistance between lid and convection wall.
4. Adding convection on the top wall.
5. Adding ceramic insulation.

### 4.2.1 Filling

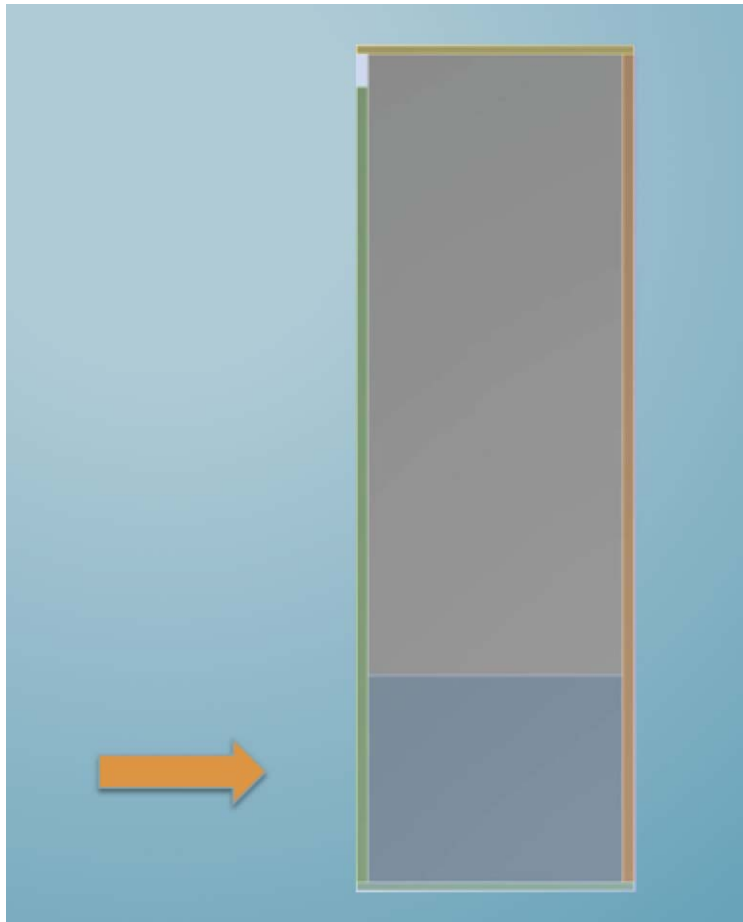
Heat transfers from combustion chamber through chamber wall to reach biomass. As thermal conductivity increases, heat should transfer more effectively through that particular material. Therefore, with a thermal conductivity of 0.17 W/m/K, biomass should experience more heat transfer once in contacted with material that has greater thermal conductivity. A total of 7 materials with thermal conductivity ranging from 0.5 to 388 W/m/K were filled at the bottom quarter of the pyrolysis chamber to verify our idea as shown in figure 4.1.

Table 4.2: filling results

	Thermal Conductivity (W/m/K)	Remaining Cellulose	
		4000 Seconds	7500 Seconds
Reference	0.17	38.93%	33.86%
Soil	0.5	37.38%	32.18%
Clay	1.1	36.75%	30.35%
Inconel 625	20	29.30%	22.32%
Carbon Steel	43	27.93%	21.39%
Nickel	92	27.74%	21.12%
Aluminum	202	26.68%	20.55%
Copper	388	25.72%	20.25%

As shown in table 4.2, results of remaining cellulose correspond to different thermal conductivities. As can be seen, while the first line is our reference value, remaining cellulose keeps decreasing as thermal conductivity increases. There will be a 40.2% increase in biomass conversion ratio when the bottom quarter is stuffed with copper.

The results are reasonable since higher thermal conductivity will transfer more heat in the same period of time, which means higher temperature for biomass to react at. However, given copper and most metal materials are expensive, filling, in general, does not provide many viable options.



*Figure 4.1: filling geometry*

#### 4.2.2 Insulating & adding fins

Attaching fins would accelerate heat transfer on the heating wall side, while insulation on the convection wall side would reduce heat loss to a minimum. Therefore, both insulation and fins are interesting ideas to simulate as shown in figure 4.2.

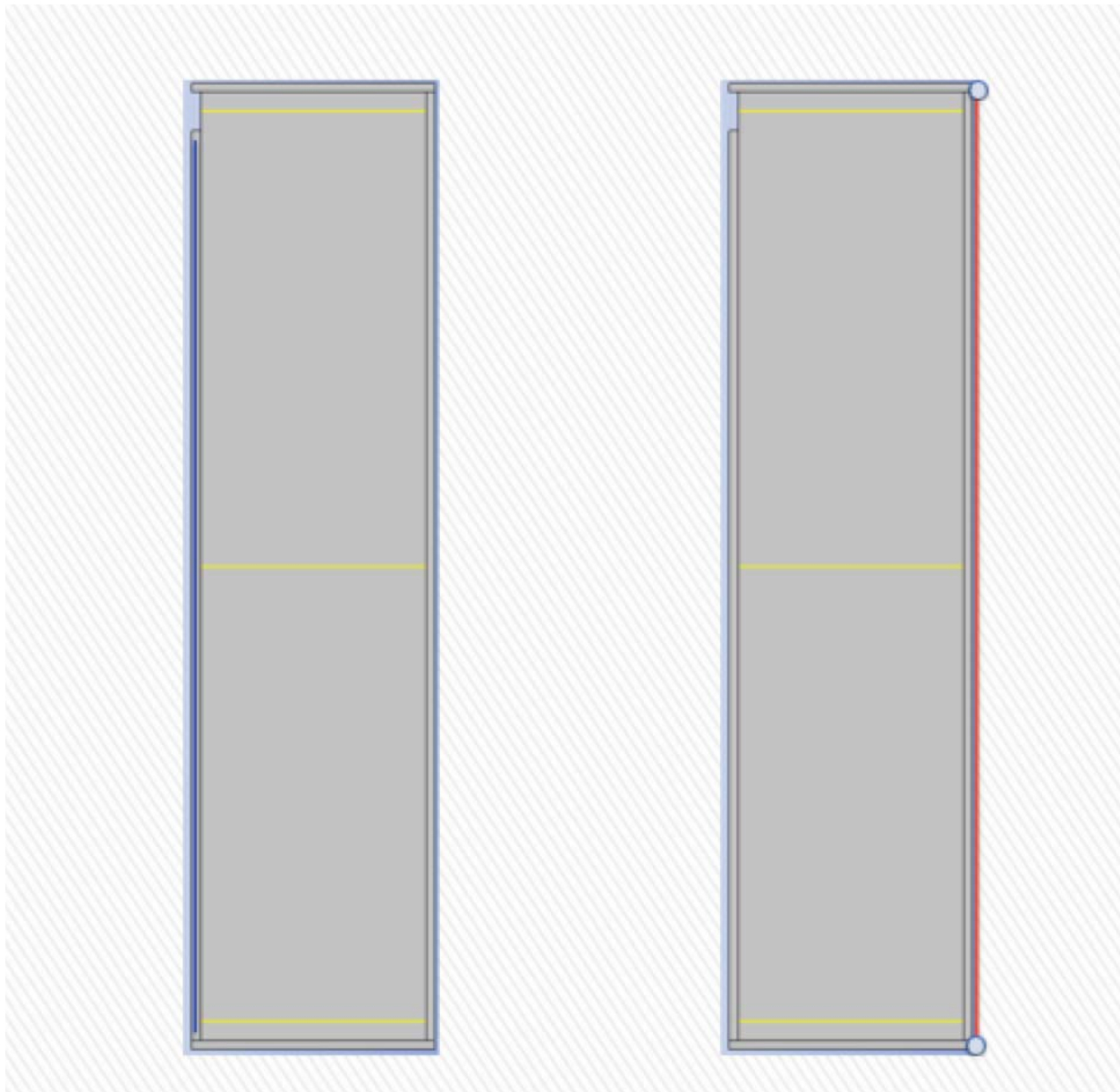


*Figure 4.2: fins and insulation*

As shown in figure 4.2, on the left hand side, the blue line indicates where the fins will be added and on the right hand side, the red line indicates where insulation is most desirable. In reality, attaching fins, essentially, would increase heat transfer coefficient. In the meanwhile, insulation would decrease heat transfer coefficient. Thus the effects of fins and insulation can be investigated simply by changing the value of heat transfer coefficient.

Table 4.2: results of fins and insulation

	Parameters		Remaining Cellulose	
			4000 seconds	7500 seconds
Reference	120 W/m <sup>2</sup> /K	20 W/m <sup>2</sup> /K	38.93%	33.86%
Fins attached	180 W/m <sup>2</sup> /K	20 W/m <sup>2</sup> /K	38.55%	33.76%
Insulation	120 W/m <sup>2</sup> /K	0 W/m <sup>2</sup> /K	1.11%	0.00%

Table 4.2 shows the results as parameters changed to simulate attaching fins and insulation. Merely a 0.3% increase in conversion ratio when fins being added, while, surprisingly, 100% conversion ratio was achieved as the convection wall reaches adiabatic condition.

Since 100% insulation is highly unlikely to reach, we will attempt to lower the heat transfer coefficient on the convection wall. Further simulation and analysis will be introduced later in this chapter.

#### 4.2.3 Adding heating effect & contact resistance

With a closer look at the actual Cook-Stove, heating wall side of the lid as the arrow indicates on the left hand of figure 4.3 should be heated as well, and there should be contact resistance between the lid and convection wall, which is shown on the right hand side of figure 4.3 with another arrow.

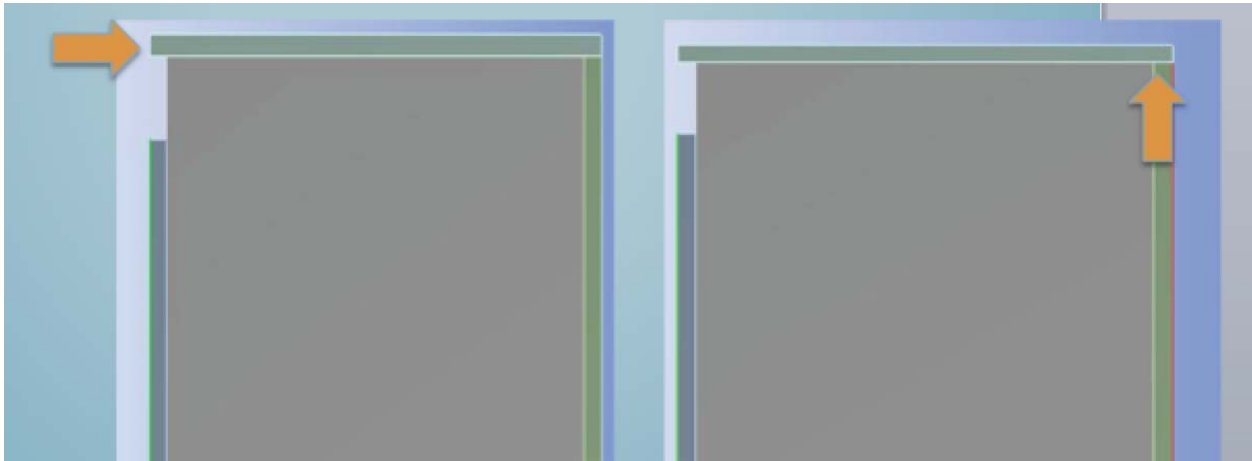


Figure 4.3 lid: heating and contact resistance

After setting the lid to a fixed temperature of 1000K and adjusting the boundary condition between lid and convection wall to no heat flux, results are shown in table 4.3.

Table 4.3: results of lid

	Conditions	Remaining Cellulose	
		4000 seconds	7500 seconds
Reference	Not applicable	38.93%	33.86%
Heating the lid	Wall temperature: 1000K	28.21%	23.59%
Contact resistance	No heat flux	38.06%	32.26%

As can be seen, there is 30.3% increase in conversion ratio once lid is heated. On the other hand, the presence of contact resistance contributes for a 4.7% increase. Both results appear reasonable. For heating the lid, higher thermal conductivity indicates that lid should heat up much faster; therefore, extra heat will transfer to biomass through the lid resulting in the increase in conversion ratio. As contact resistance is considered, it locates between the lid and the convection wall, without wasting energy to heat up the convection wall, biomass should expect more heat to react with. However, due to its location is far away from combustion chamber where little heat transfers this far to begin with, therefore, not much improvement is observed.

#### 4.2.4 Adding convection on the top wall

Originally, the boundary condition for the top wall is adiabatic, while the real situation is that there are gases flowing above the top wall. To investigate whether this flow is significant to the stove performance, boundary conditions were changed to convection, and different temperatures and heat transfer coefficients were tested.

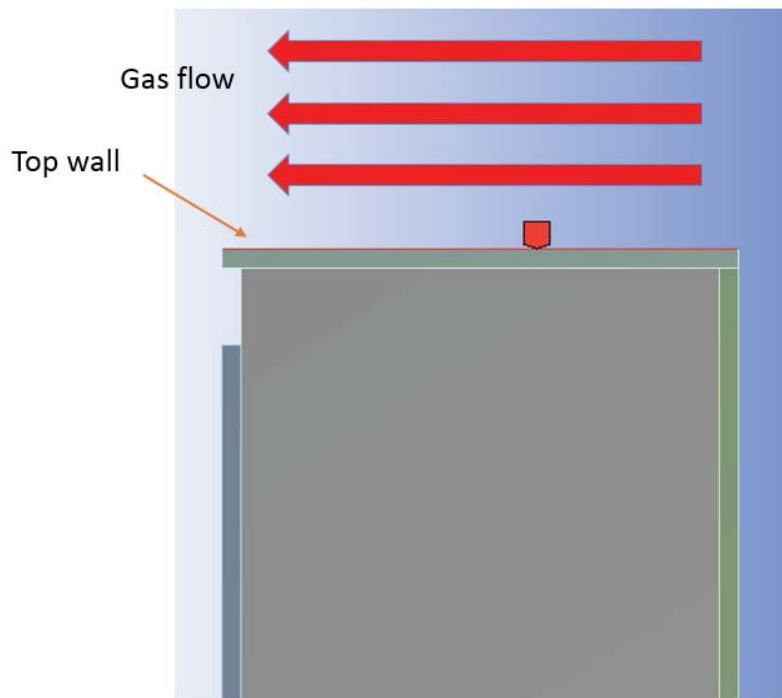


Figure 4.4: Convection on the top wall



Table 4.4: Convection on the top wall simulation results

	Conditions		Remaining Cellulose	
			4000 seconds	7500 seconds
Reference	no convection		38.93%	33.86%
top wall convection	free stream temperature (K)	heat transfer coefficient (W/m <sup>2</sup> /K)		
	300	20	40.58%	36.23%
	400	20	39.22%	34.70%
	500	20	37.52%	32.78%
	600	20	35.44%	29.67%
	700	20	32.54%	27.58%
	500	50	36.92%	32.30%

As the result shown in Table 4.4, the influence of top wall convection is only significant at high flow temperature and high heat transfer coefficient. With same heat transfer coefficient, the higher the temperature above the lid, the more cellulose can react. Similarly, with the same temperature above the lid, higher heat transfer coefficient of the lid can help decrease the remaining cellulose.

This result is reasonable because with higher temperature and higher heat transfer coefficient, more heat flux can be conducted into the chamber, so the reaction temperature can be higher. On the other hand, adding convection on the top wall is not as effective as heating the lid or adding insulation or stuffing as described in section 4.2.1 to 4.2.3.

To implement this design to the real stove, the supporting part of the lid can be porous structure so that more heat generated by the combustion can flow through the top wall

#### 4.2.5 Ceramic insulation

As introduced in 4.2.2, where the boundary condition of the convection wall is adiabatic, 100% conversion ratio can be reached. This result illustrates that insulation of convection may be an important factor for the further design. However, adiabatic condition is hard to attain in real life. In this section, we model more realistic approaches to decreasing the heat transfer coefficient on the convection wall. We attached a two centimeter ceramic insulation layer out of the convection wall.

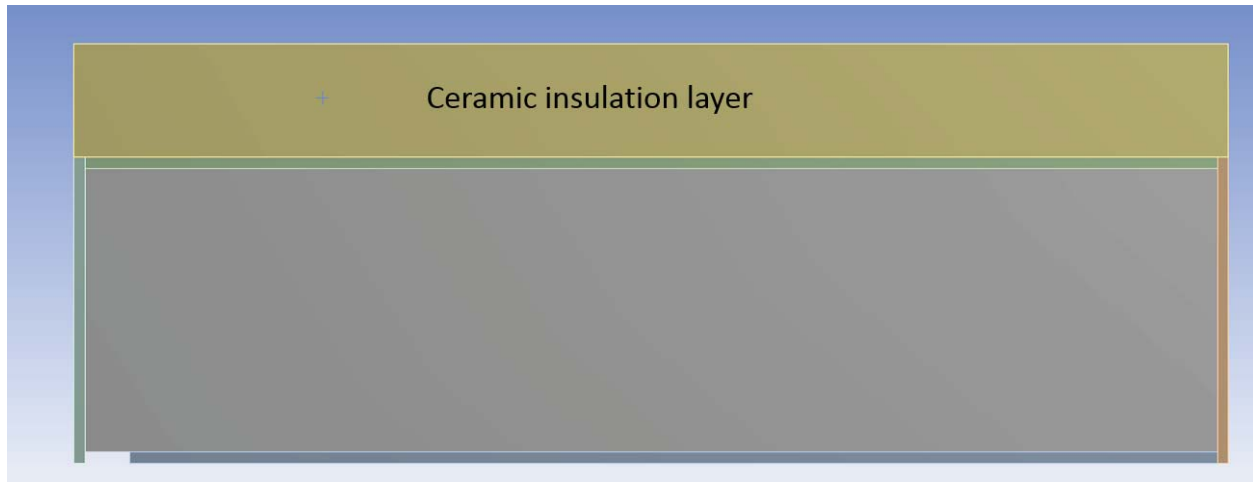


Figure 4.5: Ceramic insulation

Table 4.5: Ceramic properties (ToolBox, Ceramic material Properties, 2014)

Density (kg/m <sup>3</sup> )	Specific Heat (J/(kg*k))	Thermal Conductivity (w/(m*k))
2400	1090	1.5

Table 4.6: Simulation result

	Conditions	Remaining Cellulose	
		4000 seconds	7500 seconds
Reference	No Insulation	38.93%	33.86%
Ceramic Insulation	Thickness = 2 cm	42.10%	34.46%

However, as the result shown in Table 4.6, instead of speeding the pyrolysis reaction, insulation layer leads to a 1.5% decrease of conversion.

This is maybe because ceramic insulation layer has a high specific heat which leads to a high heat capacity, so this layer absorbs a large amount of energy which leads to less cellulose reaction.

Perform a similar heat capacity analysis as described in section 2.2 to validate the explanation above. Using the result of Table 2.1, the total heat capacity of pyrolysis chamber including four walls is

$$2332.4 + 629.7 + 2926.4 = 5888.5J/K$$

The volume of the insulation layer is:

$$V = \pi h(R_1^2 - R_2^2)$$

Where  $h$ : Height of the insulation layer,  $h = 0.204m$

$R_1$ : Outer radius of the insulation layer,  $R_1 = 0.162m$

$R_2$ : Inner radius of the insulation layer,  $R_2 = 0.142m$

And heat capacity can be obtained by the following equation.

$$C = \rho \times V \times c_p$$

Where  $C$ : Heat capacity

$\rho$ : Density of ceramic,  $\rho = 2400 \text{ kg/m}^3$

$c_p$ : Ceramic specific heat,  $c_p = 1090 \text{ J/(kg}\times\text{K)}$

The value for heat capacity is 10193 J/K, this value is nearly twice as much as the heat capacity of the whole pyrolysis chamber.

With higher heat capacity, it will take longer to heat up the insulation layer, which means the characteristic time for the ceramic insulation layer should be much bigger than 7500s.

A 30000 seconds simulation was performed to verify this reasoning, which can be considered as the time required for the insulation layer to reach heat transfer steady state.

Compared to the remaining cellulose fraction at 20000s of the reference model (30.78%), a 30000 seconds simulation with ceramic insulation layer has 24.73% remaining cellulose. This value is much lower than the reference value, which indicates that the result is reasonable.

### 4.3 Design Recommendation

After finishing all optimization ideas and analyzing all optimization results, we conclude:

1. More attention should be devoted to approaching adiabatic condition on the convection wall side.
2. Both lid heating and contact resistance should be included in any further simulation and design changes.
3. In the absence of economic concerns, filling with metals like copper should prove to be helpful in increasing final biomass conversion ratio. Clay is a more realistic choice, given its affordability and availability.
4. Convection on the top should not be a factor due to the low temperature of situation.
5. Insulation with ceramic due to its heat capacity should not be considered.

### 4.4 Future Improvement of the Model

There are still many room for improvement of this model.

First, this model doesn't include any gas source. In reality, pyrolysis reactions will generate gases such as methane and tar, which will make a significant influence to the heat transfer of the pyrolysis chamber, because this will change the heat transfer mode from conduction to convection due to the flow of the gas. Also, with the presence of the gases, the parameter of porous medium need to be specified further because they have make more affects as well. For the gas generation, it can be achieved by adding a mass source in the FLUENT with UDF. The challenge is that how to determine the temperature and direction of the generated gas. For the temperature, ideally, it should take the heat of reaction into account, but generating a gas whose temperature is equal to the local temperature would be a good start. As for direction, the density of gas product should be compared to the air originally present in the pyrolysis chamber first. Second, there is only one chemical reaction included, which is the decomposition of the cellulose. However, pyrolysis reaction is a very complicated process in which many reactions proceeds at the same

time, including more reactions will definitely influence heat generation and the temperature distribution inside the chamber.

Third, boundary conditions on the top wall and the bottom wall can be more accurate. For now, they are just adiabatic walls, but in reality, the wood feed channel near the bottom wall and the lid near the top wall can largely influence the heat conduction of both walls.

Fourth, many details of the geometry can be created more accurately. The simulation results showed that even a different boundary condition difference on one side of the top wall can make a huge difference of the simulation result. For further improvement, the heat of the top wall and the contact resistance between the top wall and the convection should be taken into consideration.

Finally, the boundary condition of the convection wall should be further specified. In the current model, the convection wall boundary condition is determined by the comparison to the experimental data, however, with the improvement of the chemical mechanism and the refinement of the geometry, the boundary condition of the convection will not match the lab data anymore. A better approach is to include the convection chamber into the model and set the boundary condition outside the convection chamber as the ambient condition. This assumption will be valid for all the situation.

## References

Chen, Y. (2011). *Design of a Biochar-Producing CookStove*. Ithaca.

Teeranai Pattanotai, H. W. (2014, 1 30). Gasification characteristic of large wood chars with anisotropic structure. *Fuel*, pp. Volme 117, Part A 331-339.

ToolBox, T. E. (2014). *Ceramic material Properties*. Retrieved from The Engineering ToolBox: [http://www.engineeringtoolbox.com/ceramics-properties-d\\_1227.html](http://www.engineeringtoolbox.com/ceramics-properties-d_1227.html)

ToolBox, T. E. (2014). *Gases - Specific Heats and Individual Gas Constants*. Retrieved from The Engineering ToolBox: [http://www.engineeringtoolbox.com/specific-heat-capacity-gases-d\\_159.html](http://www.engineeringtoolbox.com/specific-heat-capacity-gases-d_159.html)

ToolBox, T. E. (2014). *Metals - Specific Heats*. Retrieved from The Engineering ToolBox: <http://www.engineeringtoolbox.com/>

## Division of works

Haolun Fan is mainly responsible for the development of the model (except the heat source coding), such as geometry simplification, building geometry, generating mesh, and setting up boundary conditions. He is also responsible for the verification of the heat source by comparing the heat source to a hand calculation heat source. In addition, Haolun Fan is responsible for the mesh sensitivity check.

Junxing Lu is mainly responsible for the development of the UDF code, from uniform to time dependence to temperature and mass fraction dependence. In addition, he is responsible for the chamber wall validation as well as adjusting settings to approach actual situation with real data.

As for the design part, Haolun Fan and Junxing Lu discuss and propose new designs together and share the simulation work. In particular, Junxing Lu is responsible for collecting and analyzing simulation results of filling, insulating and fins, heating and contact resistance approach; Haolun Fan is responsible for collecting and analyzing simulation results of convection on the top wall and ceramic insulation approach.

### Division of writing works

	Haolun Fan	Junxing Lu
1 Introduction		+
2 Development of Model	+	
2.1 Simplification	+	
2.2 Geometry		+
2.3 Mesh	+	
2.4 Material Properties and Boundary Conditions	+	
2.5 Heat Source		+
3 Simulation results and verification	+	
3.1 Mesh sensitivity	+	
3.2 Parameter specification	+	
3.3 Simulation results	+	
3.4 Heat source verification	+	
4 Optimization		+
4.1 Objectives		+
4.2 Approaches		+
4.2.1 Filling		+
4.2.2 Insulating and fins		+
4.2.3 heating and contact resistance		+

4.2.4 Convection on the top wall	+	
4.2.5 Ceramic insulation	+	
4.3 Design Recommendation		+
4.4 Future improvement of the model	+	